Elastomers and Composites
Vol. 55, No. 4, pp. 321~328 (December 2020)

Print ISSN 2092-9676/Online ISSN 2288-7725
DOI: https://doi.org/10.7473/EC.2020.55.4.321

Synthesis of Zinc Oxide Nanoparticle-(C_{60}) Fullerene Nanowhisker Composite for Catalytic Degradation of Methyl Orange under Ultraviolet and Ultrasonic Irradiation

Jeong Won Ko[*], Yeon-A Son[*,†], and Weon Bae Ko[,***,†]**

[*]*Department of Science Education, Graduate School, Dankook University, 152, Jukjeon-ro, Suji-gu, Yongin-si, Gyeonggi-do 16890, Republic of Korea*
[**]*Department of Chemistry, Shamyook University, 815, Hwarang-ro, Nowon-gu, Seoul 01795, Republic of Korea*
[***]*Department of Convergence Science, Graduate School, Shamyook University, 815, Hwarang-ro, Nowon-gu, Seoul 01795, Republic of Korea*

(Received November 3, 2020, Revised November 23, 2020, Accepted November 25, 2020)

Abstract: Zinc nitrate hexahydrate ($Zn(NO_3)_2 \cdot 6H_2O$) and sodium hydroxide (NaOH) were dissolved in distilled water and stirred for 30 min. The resulting solution was sonicated by an ultrasonic wave for 45 min. This solution was washed with distilled water and ethanol after centrifugation; next, it was placed in an electric furnace at 200°C for 1 h under the flow of Ar gas to obtain zinc oxide nanoparticle. A zinc oxide nanoparticle-(C_{60}) fullerene nanowhisker composite was synthesized using the zinc oxide nanoparticle solution, C_{60}-saturated toluene, and isopropyl alcohol via the liquid-liquid interfacial precipitation method. The zinc oxide nanoparticle and zinc oxide nanoparticle-(C_{60}) fullerene nanowhisker composite were characterized using X-ray diffraction, scanning electron microscopy, and Raman spectroscopy, and they were used for the catalytic degradation of methyl orange (MO) under ultraviolet (at 254 and 365 nm) and ultrasonic irradiation. In addition, the catalytic degradation of MO over the zinc oxide nanoparticle and zinc oxide nanoparticle-(C_{60}) fullerene nanowhisker composite was evaluated using ultraviolet-visible spectroscopy.

Keywords: zinc oxide nanoparticle-(C_{60}) fullerene nanowhisker, methyl orange, ultraviolet, ultrasonic irradiation

Introduction

Organic dyes can cause vomiting, pain, hemorrhage, ulceration of skin and mucous membranes, and dermatitis.[1] In addition, the presence of large amounts of organic dyes in wastewater can cause the toxic environment to aquatic organisms, inhibit the penetration of sunlight, and reduce the rate of photosynthesis.[2] Therefore, the removal of organic dyes from wastewater is imperative for preserving the natural environment. MO is widely used as a coloring agent for the detection of hydrogen gas in the food, leather, and pharmaceutical industries.[3,4] Various physical (coagulation, reverse osmosis, membrane filtration), chemical (reduction, oxidation, ion exchange, complexometric), and biological (aerobic and anaerobic) methods are used for removing MO from wastewater.[5] Among these methods, photocatalytic degradation is the most efficient approach for removing dyes and other pollutants from wastewater. Photocatalytic degradation converts organic dyes completely to H_2O, CO_2, and less or nontoxic compounds without causing secondary pollution.[6]

Advanced oxidation processes are usually used for the degradation of organic dyes in wastewater.[7-10] These mechanisms involve the formation of hydroxyl (·OH) and superoxide ($\cdot O_2^-$) radicals.[11] Semiconductor metal oxides such as ZnO can act as catalysts for the degradation of organic dyes in wastewater.[2]

Zinc oxide is an n-type metal oxide semiconductor with a wide band gap of 3.37 eV and a large exciting binding energy of 60 meV at room temperature.[12] Because of these properties, ZnO is used as antibacterial agents and in solar cells, light emitting diodes, nano lasers, piezoelectric devices, ultraviolet (UV) shielding materials, and gas sensors.[7-9,13-15]

However, in ZnO, the recombination rate of photo-generated electron-hole pairs is usually faster than the surface redox reaction, which severely limits its practical use, especially in the photocatalytic degradation of organic com-

[†]Corresponding author E-mail: kowb@syu.ac.kr; yeona@dankook.ac.kr

pounds.[2] Therefore, various studies have been carried out to suppress the electron-hole pair recombination in ZnO in order to improve the photocatalytic efficiency. The commonly used approaches for suppressing the electron-hole pair recombination of ZnO include combining ZnO with other semiconductors[8-11,16,17] or carbon-based materials[18-26] and doping with metals[27-34] and nonmetals.[35-38]

When combined with carbon nanotubes[39,40] and carbon nanofibers,[41,42] ZnO shows excellent photocatalytic activity. In particular, carbon-based nanomaterials act as an electron acceptors. It acts as an electron transport materials in the photocatalytic degradation of organic dyes and facilitates the migration of photo-generated electrons and suppressing the charge recombination, thus enhances the lifetime of electron-hole pairs and improves the photocatalytic efficiency of the composite.[43]

(C_{60}) Fullerene nanowhiskers are composed of single-crystal (C_{60}) fullerene, a typical carbon nanomaterial, and thin needle-like fibers with a length less than 100 μm.[44] These nanowhiskers are used in many applications such as in chemical sensors, solar cells, photosensors, and field-effect transistors.[45-50] The nanowhiskers are prepared by the liquid–liquid interfacial precipitation (LLIP) method.[46]

(C_{60}) Fullerene nanowhiskers exhibit unique properties such as high charge carrier mobility,[51] optical transmittance,[45] and higher Young's modulus than that of the pristine (C_{60}) fullerene crystal.[52] Owing to these unique properties, (C_{60}) fullerene nanowhiskers act as excellent electronic acceptors and electron transport materials in hybrid nanocomposites.

Various efforts have been made to develop hybrid nanocomposites of semiconductor materials and (C_{60}) fullerene nanowhiskers with excellent nanocatalytic performance.[53,54]

In this study, we synthesized a zinc oxide nanoparticle-(C_{60}) fullerene nanowhisker nanocomposite from zinc oxide nanoparticles using the LLIP method.

The zinc oxide nanoparticle and zinc oxide nanoparticle-(C_{60}) fullerene nanowhisker composite were used to degrade MO under UV (at 254 and 365 nm) and ultrasonic irradiation.

Experimental

1. Materials

(C_{60}) Fullerene was obtained from Tokyo Chemical Industry Co. Ltd. MO and hydrogen peroxide (H_2O_2, 30%, w/w) were purchased from Daejung Chemicals. Zinc nitrate hexahydrate ($Zn(NO_3)_2{\cdot}6H_2O$), sodium hydroxide (NaOH), toluene (C_7H_8), ethanol (C_2H_5OH), and 2-propanol (C_3H_8O) were supplied by Samchun Chemicals.

2. Instruments

An electric furnace (Ajeon Heating Industry Co., Ltd.) was used to heat the samples. The photocatalytic degradation of MO was confirmed using ultraviolet-visible (UV-Vis) spectroscopy (Shimazu UV-1601 PC) under ultraviolet and ultrasonic radiation condition. An ultraviolet lamp(8 W, 254 nm/365 nm, 77202 Marne La Vallee-Cedex 1, France) was used for irradiation of UV light. The ultrasonic radiation of 20 kHz frequency was generated using UGI1200 (Hanil Ultrasonic Co., Ltd.), equipped with a horn-type tip of 13 nm OD. The crystal structures of the samples were analyzed using X-ray diffraction (XRD) (Bruker, D8 Advance) at 40 kV and 40 mA. Raman spectroscopy (BWTEK, BWS465-532S) was used to analyze the lattice vibrations of the sample. Scanning electron microscopy (SEM) (JEOL, Ltd., JSM-6510) measurements were carried out at an accelerating voltage of 10 kV to examine the surface morphologies of the samples.

3. Synthesis of zinc oxide nanoparticle

Zinc oxide nanoparticle was prepared by mixing 1 M zinc nitrate hexahydrate ($Zn(NO_3)_2{\cdot}6H_2O$) and 10 M of sodium hydroxide (NaOH) with 20 mL of distilled water followed by stirring for 30 min. The resulting solution was subjected to ultrasonic irradiation for 45 min. The mixture was then washed with distilled water and ethanol by centrifugation and placed in an electric furnace at 200°C for 1 h under the flow of Ar gas to obtain zinc oxide nanoparticles.

4. Preparation of the zinc oxide nanoparticle-(C_{60}) fullerene nanowhisker composite

The zinc oxide nanoparticle-(C_{60}) fullerene nanowhisker composite was prepared using the LLIP method by blending the zinc oxide nanoparticle solution (~0.2 mg/mL), C_{60}-saturated toluene (~14 mg/mL), and isopropyl alcohol at a volume ratio of 1:14:75. The resulting solution was kept at 5°C for 20 h.

5. Catalytic degradation of MO over the zinc oxide nanoparticle and zinc oxide nanoparticle-(C_{60}) fullerene nanowhisker composite

The catalytic activities of the zinc oxide nanoparticle and zinc oxide nanoparticle-(C_{60}) fullerene nanowhisker composite for the degradation of MO were evaluated. Stock MO solutions were synthesized using 2 mM of MO powder. The zinc oxide nanoparticle and zinc oxide nanoparticle-(C_{60}) fullerene nanowhisker composite (0.1 g/L) were used for the photocatalytic degradation of a 4.2×10^{-2} mM MO solution containing H_2O_2. The pH of the MO solution was maintained at 5.7, H_2O_2 was used as an oxidizing reagent. The solution was stirred for 30 min in the absence of light to attain an adsorption-desorption equilibrium between the MO molecules and the catalysts.

The catalytic degradation process was monitored using UV-Vis spectroscopy. The catalytic degradation of MO over the zinc oxide nanoparticle and zinc oxide nanoparticle-(C_{60}) fullerene nanowhisker composite was carried out under UV (at 254 and 365 nm) and ultrasonic irradiation.

Results and Discussion

1. Characterization of zinc oxide nanoparticle and zinc oxide nanoparticle-(C_{60})fullerene nanowhisker composite

The crystal structures and crystallite sizes of the zinc oxide nanoparticle and zinc oxide nanoparticle-(C_{60}) fullerene nanowhisker composite were examined using powder XRD.

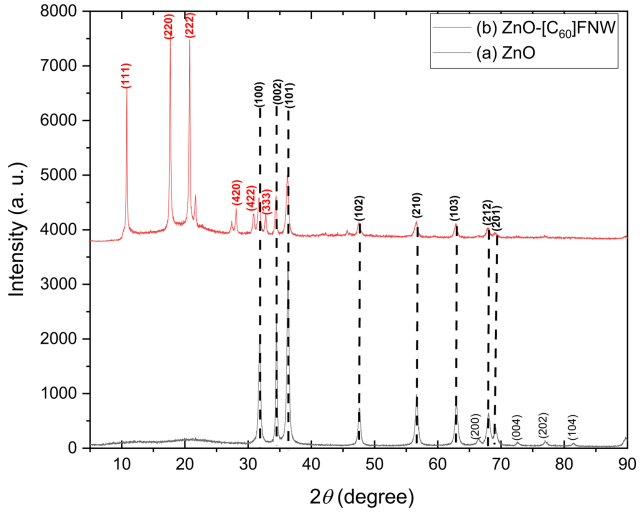

Figure 1. XRD pattern of (a) zinc oxide nanoparticle and (b) zinc oxide nanoparticle-(C_{60}) fullerene nanowhisker composite.

The XRD patterns of the zinc oxide and zinc oxide nanoparticle-(C_{60}) fullerene nanowhisker composite are shown in Figure 1. The composite showed peaks at $2\theta = 10.74°$, 17.71°, 20.69°, 28.02°, 30.79°, and 32.75° corresponding to the (111), (220), (222), (420), (422), and (333) planes of (C_{60}) fullerene nanowhisker, respectively. On the other hand, the peaks at $2\theta = 31.77°$, 34.42°, 36.26°, 47.54°, 56.61°, 62.86°, 67.39°, and 69.10° correspond to the (100), (002), (101), (102), (210), (103), (212), and (201) planes of zinc oxide nanoparticle, respectively (JCPDS card No.36-1451).[55] The XRD results indicated the successful preparation of the zinc oxide nanoparticle and zinc oxide nanoparticle-(C_{60}) fullerene nanowhisker composite. The crystallite sizes of the synthesized zinc oxide nanoparticle and zinc oxide nanoparticle-(C_{60}) fullerene nanowhisker composite were calculated using the Scherrer formula as follows:

$$D = k \cdot \lambda / \beta \cdot \cos\theta$$

where D is the crystallite size, λ is the wavelength of Cu-Kα radiation ($\lambda = 0.154$ nm), k is the Scherrer constant (taken as 0.94), 2θ is the angle between the incident and scattered X-rays, and β is the full width at half maximum. The average crystallite size of the zinc oxide nanoparticle was found to be approximately 21.04 nm (Table 1).

Figure 2 shows the morphologies of the zinc oxide nanoparticle and zinc oxide nanoparticle-(C_{60}) fullerene nanowhisker composite photographed using SEM. The image of SEM revealed that most of the synthesized zinc oxide nanoparticle structure showed almost snow flower-like morphology in Figure 2(a). In the zinc nanoparticle-(C_{60}) fullerene nanowhisker composite, with snow flower-like structure and agglomerated zinc oxide nanoparticle were observed on

Table 1. Crystallite Size of Zinc Oxide Nanoparticle, as Estimated Using the Scherrer Equation

Miller Indices (*hkl*)	Diffraction angle 2θ (degree)	FWHM (β) (degree)	Crystallite size (nm)
(100)	31.77	0.373	23.14
(002)	34.42	0.295	29.46
(101)	36.26	0.400	21.84
(102)	47.54	0.477	19.02
(210)	56.61	0.529	17.82
(103)	62.86	0.493	19.73
(212)	67.39	0.535	18.65
(201)	69.10	0.540	18.67
Average			21.04

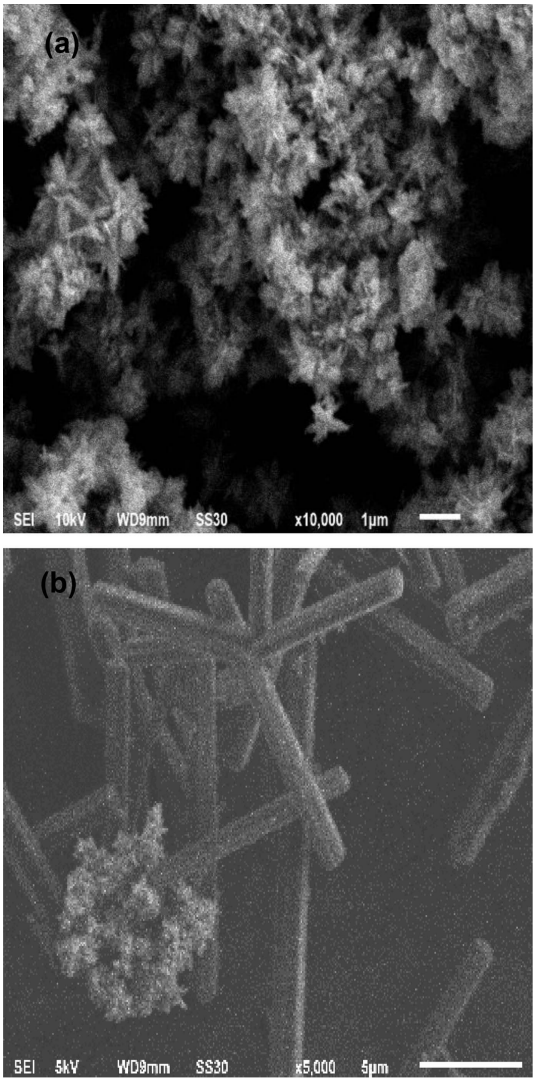

Figure 2. SEM image of (a) zinc oxide nanoparticle and (b) zinc oxide nanoparticle-(C_{60}) fullerene nanowhisker composite.

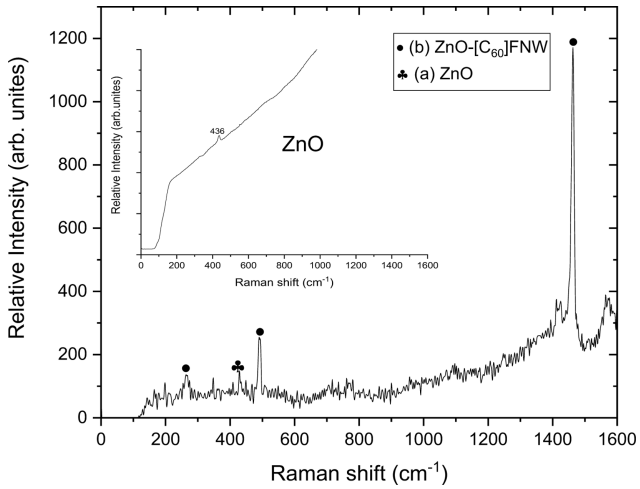

Figure 3. Raman spectrum of (a) zinc oxide nanoparticle and (b) zinc oxide nanoparticle-(C_{60}) fullerene nanowhisker composite.

the (C_{60}) fullerene nanowhisker with a needle-like structure in Figure 2(b).

The vibrational modes of the zinc oxide nanoparticle and zinc oxide nanoparticle-(C_{60}) fullerene nanowhisker compos-

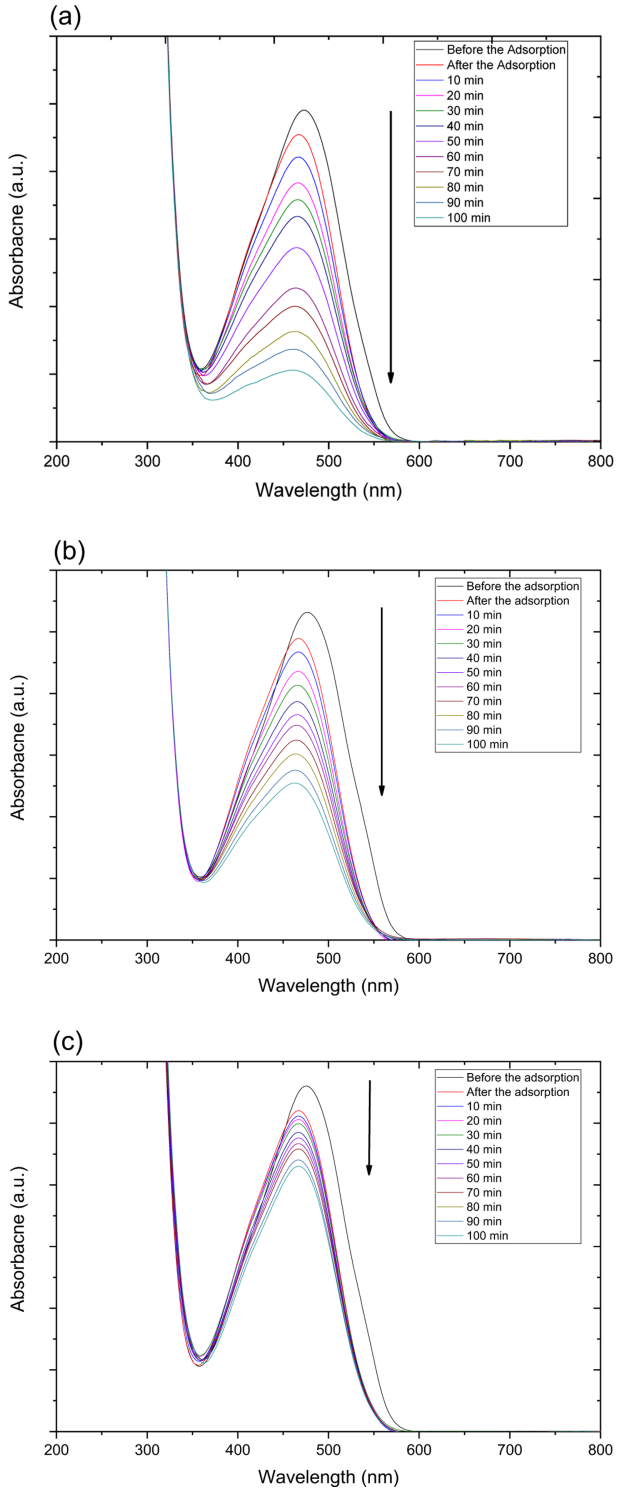

Figure 4. UV-vis spectra for catalytic degradation of MO using on zinc oxide nanoparticle under UV light (a) at 254 nm, (b) 365 nm, and (c) ultrasonic irradiation.

ite were observed using Raman spectroscopy, as shown in Figure 3.

The zinc oxide nanoparticle-(C_{60}) fullerene nanowhisker composite showed $H_g(1)$, $A_g(1)$, and $A_g(2)$ Raman shifts at 263, 490, and 1460 cm^{-1}, respectively because of the presence of (C_{60}) fullerene nanowhisker. A peak corresponding to the E_{2h} mode of the zinc oxide nanoparticle was observed at 436 cm^{-1}.[56] The peak shown at 430 cm^{-1} can be seen as the presence of zinc oxide nanoparticle because blue shift is generated by the (C_{60}) fullerene nanowhisker.

2. Catalytic degradation of MO with different conditions using on zinc oxide nanoparticle and zinc oxide nanoparticle-(C_{60}) fullerene nanowhisker composite

The catalytic degradation rate of MO shows in the presence of zinc oxide nanoparticle under various conditions such

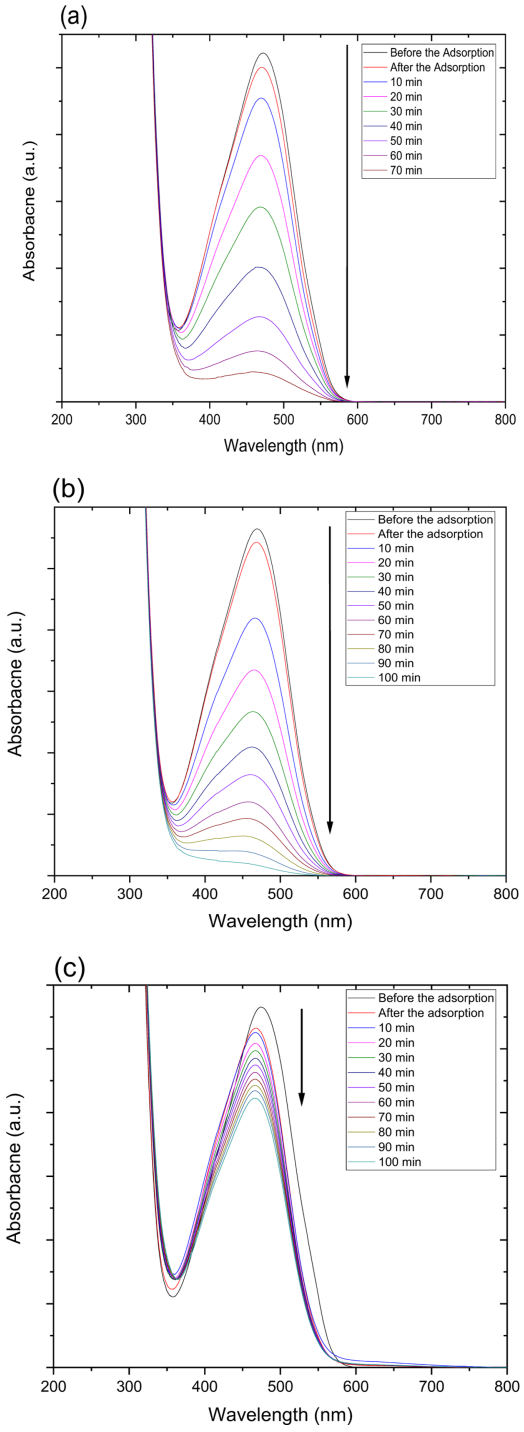

Figure 5. UV-vis spectra for catalytic degradation of MO using on zinc oxide nanoparticle-(C_{60}) fullerene nanowhisker composite under UV light (a) at 254 nm, (b) 365 nm, and (c) ultrasonic irradiation.

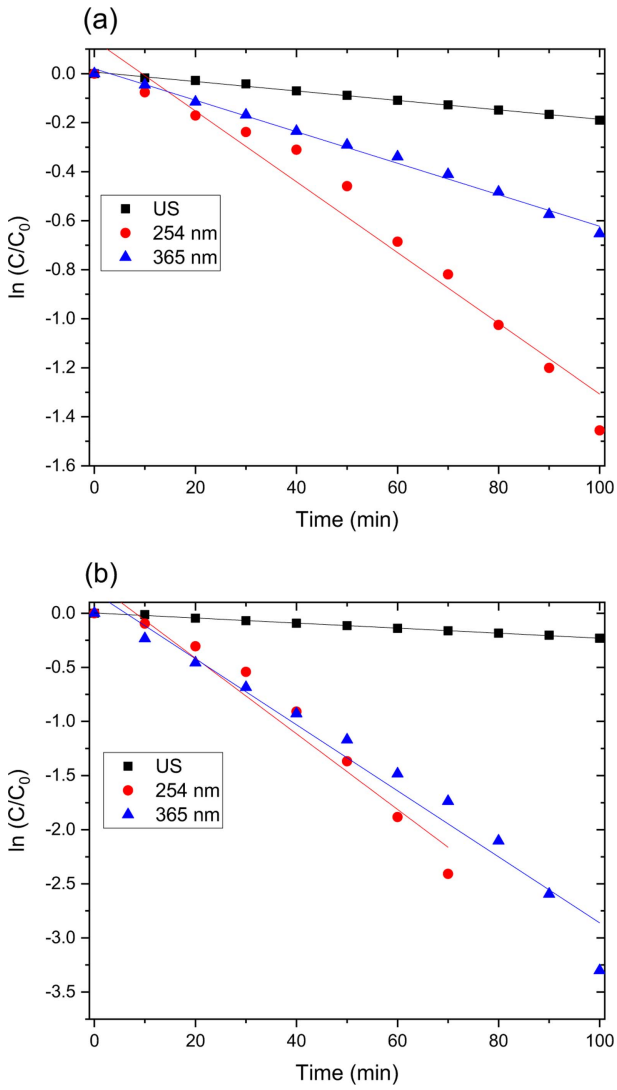

Figure 6. Kinetics study for degradation of MO using on (a) zinc oxide nanoparticle and (b) Zinc oxide nanoparticle-(C_{60}) fullerene nanowhisker composite as a catalyst under UV irradiation at 254 nm, 365 nm, and ultrasonic irradiated condition.

as UV and ultrasonic irradiation in Figure 4. The MO degradation rate under various conditions decreased in the following order: 254 nm UV irradiation > 365 nm UV irradiation > ultrasonic irradiation.

Also, catalytic degradation rate of MO using on zinc oxide nanoparticle-(C_{60}) fullerene nanowhisker composite exhibits in Figure 5. The tendency of MO degradation rate under various conditions in Figure 5 decreased similarly to zinc oxide nanoparticle catalyst in the following order: 254 nm UV irradiation > 365 nm UV irradiation > ultrasonic irradiation.

3. Kinetics study for the degradation of MO over the zinc oxide nanoparticle and zinc oxide nanoparticle-(C_{60}) fullerene nanowhisker composite as catalysts

Figure 4 and 5 show the UV-Vis spectra for the catalytic degradation of MO over the zinc oxide nanoparticle and zinc oxide nanoparticle-(C_{60}) fullerene nanowhisker composite as catalysts. As can be observed from Figure 6, the R^2 values (coefficient of determination) for the pseudo first-order reaction kinetics were 0.997, 0.995, and 0.989. The catalytic degradation of MO was carried out under UV light (at 254 and 365 nm) and ultrasonic irradiation. The equation for the first-order reaction kinetics is as follows (Figure 6):

$$(dC/dt) = -k_1 C$$

where C is the initial azo dye concentration and k_1 is the first-order rate constant. The linear behavior of the curves indicates that the catalytic degradation of MO over the catalysts followed pseudo first-order kinetics.[57]

Conclusions

A zinc oxide nanoparticle-(C_{60}) fullerene nanowhisker composite was prepared via the LLIP method using a zinc oxide nanoparticle solution and saturated (C_{60}) fullerene in toluene and isopropyl alcohol. The hybrid nanocomposite was characterized using XRD, SEM, and Raman spectroscopy. The zinc oxide nanoparticle and zinc oxide nanoparticle-(C_{60}) fullerene nanowhisker composite were used for the catalytic degradation of MO under UV (254 and 365 nm) and ultrasonic irradiation. The ZnO nanoparticle-(C_{60}) fullerene nanowhisker composite showed better catalytic activity than the zinc oxide nanoparticle. The (C_{60}) fullerene nanowhiskers in the composite acted as electron acceptors and electron transfer materials during the catalytic degradation of MO, thereby improved the efficiency of the composite. The MO degradation rate of the composite under various conditions decreased in the following order: 254 nm UV irradiation > 365 nm UV irradiation > ultrasonic irradiation. Overall, the zinc oxide nanoparticle-(C_{60}) fullerene nanowhisker composite showed better catalytic degradation of MO than the ZnO nanoparticles. In addition, the kinetics of the catalytic degradation of MO over the hybrid catalyst followed the pseudo-first-order reaction rate law.

References

1. C. Lavanya, D. Rajesh, C. Sunil, and S. Sarita, “Degradation of toxic dyes: A review”, *Int. J. Curr. Microbiol. Appl. Sci.*, **3**, 189 (2014).
2. V. N. Nguyen, D. T. Tran, M. T. Nguyen, T. T. T. Le, M. N. Ha, M. V. Nguyen, and T. D. Pham, “Enhanced photocatalytic degradation of methyl orange using ZnO/graphene oxide nanocomposites”, *Res. Chem. Intermed.*, **44**, 3081 (2018).
3. T. Katsuda, H. Ooshima, M. Azuma, and J. Kato, “New detection method for hydrogen gas for screening hydrogen-producing microorganisms using water-soluble Wilkinson's catalyst derivative”, *J. Biosci. Bioeng.*, **102**, 220 (2006).
4. B. Choudhary, A. Goyal, and S. L. Khokra, “New visible spectrophotometric method for estimation of itopride hydrochloride from tablets formulations using methyl orange reagent”, *Int. J. Pharm. Pharm. Sci*., **1**, 159 (2009).
5. Y. M. Slokar and A. M. Le Marechal, “Methods of decoloration of textile wastewaters”, *Dyes Pigm*., **37**, 335 (1998).
6. D. Chatterjee and S. Dasgupta,“Visible light induced photocatalytic degradation of organic pollutants”, *J. Photochem. Photobiol. C*, **6**, 186 (2005).
7. M. Seo, Y. Jung, D. Lim, D. Cho, and Y. Jeong, “Piezoelectric and field emitted properties of controlled ZnO nanorods on CNT yarns”, *Mater. Lett.*, **92**, 177 (2013).
8. R. Li, S. Yabe, M. Yamashita, S. Momose, S. Yoshida, S. Yin, and T. Sato, “Synthesis and UV-shielding properties of ZnO- and CaO-doped CeO_2 via soft solution chemical process”, *Solid State Ion.*, **151**, 235 (2002).
9. C. Y. Zhang, “The influence of post-growth annealing on optical and electrical properties of p-type ZnO films”, *Mater. Sci. Semicond. Process.*, **10**, 215 (2007).
10. Q. Xiao, and L. Ouyang, “Photocatalytic photodegradation of xanthate over $Zn_{1-x}Mn_xO$ under visible light irradiation”, *J. Alloys Compd.*, **479**, L4 (2009).
11. M. Purica, E. Budianu, and E. Rusu, “ZnO thin films on semiconductor substrate for large area photodetector applications”, *Thin Solid Films*, **383**, 284 (2001).

12. C. S. Lin, C. C. Hwang, W. H. Lee, and W. Y. Tong, "Preparation of zinc oxide (ZnO) powders with different types of morphology by a combustion synthesis method", *Mater. Sci. Eng. B. Solid State Mater. Adv. Technol.*, **140**, 31 (2007).
13. N. Talebian, S. M. Amininezhad, and M. Doudi, "Controllable synthesis of ZnO nanoparticles and their morphology-dependent antibacterial and optical properties", *J. Photochem. Photobiol. B*, **120**, 66 (2013).
14. L. Zhong, L. and K. Yun, "Graphene oxide-modified ZnO particles: synthesis, characterization, and antibacterial properties", *Int. J. Nanomedicine*, **10**, 79 (2015).
15. A.Yu, J. Qian, H. Pan, Y. Cui, M. Xu, L. Tu, and X. Zhou, "Micro-lotus constructed by Fe-doped ZnO hierarchically porous nanosheets: preparation, characterization and gas sensing property", *Sens. Actuators B Chem.*, **158**, 9 (2011).
16. T. J. Kuo, C. N. Lin, C. L. Kuo, and M. H. Huang, "Growth of ultralong ZnO nanowires on silicon substrates by vapor transport and their use as recyclable photocatalysts", *Chem. Mater.*, **19**, 5143 (2007).
17. P. Sathishkumar, R. Sweena, J. J. Wu, and S. Anandan, S. "Synthesis of CuO-ZnO nanophotocatalyst for visible light assisted degradation of a textile dye in aqueous solution", *Chem. Eng. J.*, **171**, 136 (2011).
18. M. Azarang, A. Shuhaimi, R. Yousefi, A. M. Golsheikh, and M. Sookhakian, " Synthesis and characterization of ZnO NPs/reduced graphene oxide nanocomposite prepared in gelatin medium as highly efficient photo-degradation of MB", *Ceram. Int.*, **40**, 10217 (2014).
19. T. Xu, L. Zhang, H. Cheng, and Y. Zhu,"Significantly enhanced photocatalytic performance of ZnO via graphene hybridization and the mechanism study", *Appl. Catal. B*, **101**, 382 (2011).
20. Z. Tian, S. Bai, K. Cao, and J. Li, "Facile preparation of ZnO nanorods/reduced graphene oxide nanocomposites with photocatalytic property", *Mater. Express*, **6**, 437 (2016).
21. D. Li, W. Wu, Y. Zhang, L. Liu, and C. Pan, "Preparation of ZnO/graphene heterojunction via high temperature and its photocatalytic property", *J. Mater. Sci.*, **49**, 1854 (2014).
22. J. O. Hwang, D. H. Lee, J. Y. Kim, T. H. Han, B. H. Kim, M. Park, and S. O. Kim, "Vertical ZnO nanowires/graphene hybrids for transparent and flexible field emission", *J. Mater. Chem.*, **21**, 3432 (2011).
23. N. Jain, A. Bhargava, and J. Panwar, "Enhanced photocatalytic degradation of methylene blue using biologically synthesized "protein-capped" ZnO nanoparticles", *Chem. Eng. J.*, **243**, 549 (2014).
24. J. Lin, M. Penchev, G. Wang, R. K. Paul, J. Zhong, X. Jing, and C. S. Ozkan, "Heterogeneous graphene nanostructures: ZnO nanostructures grown on large-area graphene layers", *Small*, **6**, 2448 (2010).
25. R. Atchudan, T. N. J. I. Edison, S. Perumal, D. Karthikeyan, and Y. R. Lee, "Facile synthesis of zinc oxide nanoparticles decorated graphene oxide composite via simple solvothermal route and their photocatalytic activity on methylene blue degradation", *J. Photochem. Photobiol. B*, **162**, 500 (2016).
26. R. K. Biroju, P. K. Giri, S. Dhara, K. Imakita, and M. Fujii, "Graphene-assisted controlled growth of highly aligned ZnO nanorods and nanoribbons: growth mechanism and photoluminescence properties", *ACS Appl. Mater. Interfaces*, **6**, 377 (2014).
27. S. Gao, X. Jia, S. Yang, Z. Li, and K. Jiang, "Hierarchical Ag/ZnO micro/nanostructure: green synthesis and enhanced photocatalytic performance", *J. Solid State Chem.*, **184**, 764 (2011).
28. T. Jia, W. Wang, F. Long, Z. Fu, H. Wang, and Q. Zhang, "Fabrication, characterization and photocatalytic activity of La-doped ZnO nanowires", *J. Alloys Compd.*, **484**, 410 (2009).
29. J. Z. Kong, A. D. Li, H. F. Zhai, Y. P. Gong, H. Li, and D. Wu, "Preparation, characterization of the Ta-doped ZnO nanoparticles and their photocatalytic activity under visible-light illumination", *J. Solid State Chem.*, **182**, 2061 (2009).
30. S. Pyne, G. P. Sahoo, D. K. Bhui, H. Bar, P. Sarkar, S. Samanta, and A. Misra, "Enhanced photocatalytic activity of metal coated ZnO nanowires", *Spectrochim. Acta A Mol. Biomol. Spectrosc.*, **93**, 100 (2012).
31. J. H. Sun, S. Y. Dong, J. L. Feng, X. J. Yin, and X. C. Zhao, "Enhanced sunlight photocatalytic performance of Sn-doped ZnO for Methylene Blue degradation", *J. Mol. Catal. A Chem.*, **335**, 145 (2011).
32. B. Thongrom, P. Amornpitoksuk, S. Suwanboon, and J. Baltrusaitis, "Photocatalytic degradation of dye by Ag/ZnO prepared by reduction of Tollen's reagent and the ecotoxicity of degraded products", *Korean J. Chem. Eng.*, **31**, 587 (2014).
33. Z. Barzgari, A. Ghazizadeh, A., and S. Z. Askari, "Preparation of Mn-doped ZnO nanostructured for photocatalytic degradation of Orange G under solar light", *Res. Chem. Intermed.*, **42**, 4303 (2016).
34. C. Yu, K. Yang, Y. Xie, Q. Fan, C. Y. Jimmy, Q. Shu, and C. Wang, "Novel hollow Pt-ZnO nanocomposite microspheres with hierarchical structure and enhanced photocatalytic activity and stability", *Nanoscale*, **5**, 2142 (2013).
35. S. Ahmad, M. Kharkwal, and R. Nagarajan,"Application of $KZnF_3$ as a single source precursor for the synthesis of nanocrystals of ZnO_2: F and ZnO: F; synthesis, characterization, optical, and photocatalytic properties", *J. Phys. Chem. C*, **115**, 10131 (2011).
36. F. Barka-Bouaifel, B. Sieber, N. Bezzi, J. Benner, P. Roussel, L. Boussekey, and R. Boukherroub,"Synthesis and photocat-

alytic activity of iodine-doped ZnO nanoflowers", *J. Mater. Chem.*, **21**, 10982 (2011).
37. C. Shifu, Z. Wei, Z. Sujuan, and L. Wei, "Preparation, characterization and photocatalytic activity of N-containing ZnO powder", *Chem. Eng. J.*, **148**, 263 (2009).
38 S. Liu, C. Li, J. Yu, and Q. Xiang, "Improved visible-light photocatalytic activity of porous carbon self-doped ZnO nanosheet-assembled flowers", *Cryst. Eng. Comm.*, **13**, 2533 (2011).
39. X. Wang, S. Yao, and X. Li, "Sol-gel Preparation of CNT/ZnO Nanocomposite and Its Photocatalytic Property", *Chin. J. Chem.*, **27**, 1317 (2009).
40. L. P. Zhu, G. H. Liao, W. Y. Huang, L. L. Ma, Y. Yang, Y. Yu, and S. Y. Fu, "Preparation, characterization and photocatalytic properties of ZnO-coated multi-walled carbon nanotubes", *Mater. Sci. Eng. B. Solid State Mater. Adv. Technol.*, **163**, 194 (2009).
41. J. Mu, C. Shao, Z. Guo, Z. Zhang, M. Zhang, P. Zhang, and Y. Liu, "High photocatalytic activity of ZnO-carbon nanofiber heteroarchitectures", *ACS Appl. Mater. Interfaces*, **3**, 590 (2011).
42. Y. Yan, T. Chang, P. Wei, S. Z. Kang, and J. Mu, "Photocatalytic activity of nanocomposites of ZnO and multi-walled carbon nanotubes for dye degradation", *J. Dispers. Sci. Technol.*, **30**, 198 (2009).
43. P. Wang, Y. Zhai, D. Wang, and S. Dong, "Synthesis of reduced graphene oxide-anatase TiO_2 nanocomposite and its improved photo-induced charge transfer properties", *Nanoscale*, **3**, 1640 (2011).
44. J. W. Ko, S. Jeon, and W. B. Ko, "Catalytic activity of nickel (II) oxide nanoparticle-(C_{60}) fullerene nanowhisker composite for reduction of 4-nitroaniline", *Fuller. Nanotub. Carb. N.*, **28**, 1 (2020).
45. K. Miyazawa, "Synthesis of Fullerene Nanowhiskers using the liquid–liquid Interfacial Precipitation Method and their Mechanical, Electrical and Superconducting Properties", *Sci. Technol. Adv. Mater.,* **16**, 013502 (2015).
46. H. Takeya, K. Miyazawa, R. Kato, T. Wakahara, T. Ozaki, H. Okazaki, T. Yamaguchi, and Y. Takano, "Superconducting fullerene nanowhiskers", *Molecules*, **17**, 4851 (2012).
47. H. Takeya, R. Kato, T. Wakahara, K. Miyazawa, T. Yamaguchi, T. Ozaki, H. Okazaki, and Y. Takano, "Preparation and superconductivity of potassium-doped fullerene nanowhisker", *Mater. Res. Bull.*, **48**, 343 (2013).
48. V. Krishnan, Y. Kasuya, Q. Ji, M. Sathish, L. K. Shrestha, S. Ishihara, K. Minami, H. Morita, T. Yamazaki, N. Hanagata, K. Miyazawa, S. Acharya, W. Nakanishi, J. P. Hill, and K. Ariga, "Vortex-aligned fullerene nanowhiskers as a scaffold for orienting cell growth", *ACS Appl. Mater. Interfaces*, **7**, 15667 (2015).
49. K. Minami, Y. Kasuya, T. Yamazaki, Q. Ji, W. Nakanishi, J. P. Hill, H. Sakai, and K. Ariga, "Highly ordered 1D fullerene crystals for concurrent control of macroscopic cellular orientation and differentiation toward large-scale tissue engineering', *Adv. Mater.*, **27**, 4020 (2015).
50. T. Konno, C. Hirata, E. H. M. Ferreira, L. Ren, G. Piao, J. M. J. Garcia, F. M. Suarez, S. J. J. Sandoval, T. Wakahara, and K. Miyazawa, "Precise Raman measurements of C_{60} fullerene nanowhiskers synthesized using the liquid-liquid interfacial precipitation method", *Trans. Mat. Res. Soc. Japan.*, **41**, 289 (2016).
51. B. H. Cho, K. B. Lee, K. I. Miyazawa, and W. B. Ko, "Preparation of Fullerene (C_{60}) Nanowhisker-ZnO Nanocomposites by Heat Treatment and Photocatalytic Degradation of Methylene Blue", *Asian J. Chem.*, **25**, 8027 (2013).
52. R. Kato and K. Miyazawa, "Raman Laser Polymerization of C_{60} Nanowhiskers", *J. Nanomater.* **2012**, 101243 (2012).
53. J. W. Ko and W. B. Ko, "Catalytic Activity for Reduction of 4-Nitrophenol with (C_{60})Fullerene Nanowhisker-Silver Nanoparticle Composites", *Mater. Trans.*, **57**, 2122 (2016).
54. J. W. Ko and W. B. Ko, "Preparation of (C_{60})fullerene nanowhisker-silver nanoparticle composites and their catalytic activities for the oxidation of tetramethylbenzidine with hydrogen peroxide", *Fuller. Nanotub. Car. N.*, **26**, 851 (2018).
55. H. W. Yu, J. Wang, C. J. Xia, X. A. Yan, and P. F. Cheng, "Template-free hydrothermal synthesis of Flower-like hierarchical zinc oxide nanostructures", *Optik*, **168**, 778 (2018).
56. M. G. B. M. Šćepanović, M. Grujić-Brojčin, K. Vojisavljević, S. Bernik, and T. Srećković, "Raman study of structural disorder in ZnO nanopowders", *J. Raman Spectrosc.*, **41**, 914 (2010).
57. N. A. Youssef, S. A. Shaban, F. A. Ibrahim, and A. S. Mahmoud, "Degradation of methyl orange using Fenton catalytic reaction", *Egypt. J. Pet.*, **25**, 317 (2016).